Incorporating DC–DC Boost Converters in Power Flow Studies

Hamideh Feyzi[a], Reza Gholizadeh-Roshanagh[b], Mehran Sabahi[a,*], Sajad Najafi-Ravadanegh[c]

[a]*Department of Electrical Engineering, Faculty of Electrical and Computer Engineering, University of Tabriz, Tabriz 5166616471, Iran;*
[b]*Young Researchers and Elite Club, Ahar Branch, Islamic Azad University, Ahar, Iran;*
[c]*Smart Distribution Grid Research Laboratory, Department of Electrical Engineering, Faculty of Engineering, Azarbaijan Shahid Madani University, Tabriz, Iran*

Abstract

Power electronic interfaces (PEI) play an important role in future power systems. From planning and operation perspectives, there is a need to model PEIs for power flow applications. In this paper, precise modeling of a DC-DC boost converter for load flow analysis is presented, which can be generalized for other kinds of PEIs. As an application, the presented model is employed for uncertainty analysis of systems, considering uncertainty in wind power generation. The simulations are performed on a wind farm DC distribution network. The results demonstrate the robustness of the presented load flow algorithm.

Keywords: Boost converter; DC-DC converter; distribution network; power flow analysis; wind farm; uncertainty

1. Introduction

Power electronics technologies have a wide range of applications [1], particularly for modern medium [2] and low voltage [3] electric power distribution networks. Various examples can be given. They can be used as interfaces for dispersed power generation [4, 5] such as wind turbines (WT) [6], photovoltaic modules [7], and fuel cells [8]. They can be used as distribution FACTS (D-FACTS) devices for power quality enhancement [9]. Power electronics transformers are another example [10]. Power electronics devices have been touted as the main components of future microgrids [11]. Moreover, power electronics technologies play an important role in the low voltage direct current (LVDC) system, which is a planning strategy for modern low voltage distribution networks [3, 12].

Planning and operation studies in distribution networks require the modeling of power electronics devices. Several works in the literature present the modeling of D-FACTS devices, for power flow analysis, such as [13–16]. However, works on the modeling of power electronics interfaces for power flow analysis are less common, for example [17–19]. The authors in [13] modeled a unified power quality conditioner (UPQC) in order to incorporate backward-forward

sweep (BFS) power flow analysis. In [14], the authors incorporated a model of an active power conditioner (APC) in BFS algorithm and applied it to optimal location and sizing of APCs in a distribution network. Voltage control devices such as a thyristor controlled series compensator (TCSC) for distribution networks were modeled and incorporated in power flow analysis in [15]. Moreover, in [16], a line flow based power flow algorithm was proposed in order to model D-FACTS. In [17] the authors modeled voltage source converter (VSC) based interfaces for unified three-phase power flow analysis and the authors in [18, 19] modeled a DC-DC boost converter as interface for wind farms and incorporated Newton-Raphson power flow analysis.

The presented work in [18] might be of great interest for future studies on incorporating DC-DC boost converters in distribution networks, but the proposed work is not without deficiencies. Some equations are mistaken and some constant parameters are not given, such as initial values for power flow variables, and curve fitting constants etc. In this paper, we carefully investigate the modeling of a DC-DC boost converter. As an application, the load flow model of the DC-DC boost converter is incorporated in statistical analysis of a power system in which wind power generation is uncertain in nature.

The paper is organized in 8 sections. In sections 2, 3 and 4 the DC-DC boost converter is modeled for DC power flow analysis. The modeling of uncertainty in wind power generation is presented in section 5. A numerical example is given in section 6 and the concluding remarks are delivered

---

*Corresponding author
Email addresses:* `h.feyzi92@ms.tabrizu.ac.ir` (Hamideh Feyzi),
`r_gholizadeh@iau-ahar.ac.ir` (Reza Gholizadeh-Roshanagh),
`sabahi@tabrizu.ac.ir` (Mehran Sabahi), `s.najafi@azaruniv.edu`
(Sajad Najafi-Ravadanegh)

in section 7. There are also two appendices in section 8.

2. DC-DC Boost Converter

A boost or step-up converter can be modeled as power loss between input and output buses as in [20]:

$$P_{Loss} = P_L + P_{con,sw} + P_{con,D} + P_{sw,SW} + P_{sw,D} \qquad (1)$$

$$P_L = \frac{1}{T_s} \int_o^{(D+D')T_s} (R_L I_{in}) i_{in}(t) \cdot dt = R_L I_{in}^2 \qquad (2)$$

$$P_{con,sw} = \frac{1}{T_s} \int_o^{DT_s} (V_{o,sw} + R_{o,sw} I_{in}) i_{in}(t) \cdot dt = \frac{D}{D+D'} (V_{o,sw} + R_{o,sw} I_{in}) I_{in} \qquad (3)$$

$$P_{con,D} = \frac{1}{T_s} \int_{DT_s}^{(D+D')T_s} (V_{o,D} + R_{o,D} I_{in}) i_{in}(t) \cdot dt = \frac{D'}{D+D'} (V_{o,D} + R_{o,D} I_{in}) I_{in} \qquad (4)$$

$$P_{sw,SW} = \frac{A_{on,sw} + A_{off,sw}}{T_s} V_{out} I_{in} \qquad (5)$$

$$P_{sw,D} = \frac{A_{rec,D}}{T_s} V_{out} I_{in} \qquad (6)$$

where: D—relative conducting time for the IGBT, D'—relative conducting time for the diode, R_L—resistance of the inductor, $V_{o,sw}$—constant voltage drop in IGBT, $R_{o,sw}$—conducting resistance in IGBT, $V_{o,D}$—constant voltage drop in diode, $R_{o,D}$—conducting resistance in diode, $A_{on,sw}$—turn-on curve fitting constants for the IGBT, $A_{off,sw}$—turn-off curve fitting constants for the IGBT, $A_{rec,D}$—turn-off curve fitting constants for the diode, T_s—switching period time.

The relative conducting time D and D' is obtained by:

$$D = \sqrt{\frac{2LI_i}{T_s} \frac{D_z}{D_x D_y}} \qquad (7)$$

$$D' = \frac{2LI_i}{D_x DT_s} - D \qquad (8)$$

where:

$$D_x = V_i - I_i(R_L + R_{o,sw}) - V_{o,sw}$$

$$D_y = I_i(R_{o,D} - R_{o,sw}) - V_{o,sw} + V_{o,D} + V_j$$

$$D_z = -V_i + I_i(R_L + R_{o,D}) + I_j R_{o,D} + V_{o,D} + V_j$$

3. Results DC Power Flow Analysis

DC power flow is used for a distribution network containing DC-DC converters. The generalized equation for bus (node) voltage is shown in (9) [18]:

$$V_k = \frac{1}{G_{kK}} \left(\frac{P_k}{V_k} - \sum_m G_{km} V_m \right) \qquad (9)$$

where: V_k—bus (node) voltage, P_k—nodal power, G_{km}—node admittance.

The node voltage is adjusted iteratively using (10) until the final solution is obtained. In this paper, the Newton-Raphson (N-R) method which is used to solve the AC systems is adopted for the DC systems [18]. Only two variables are necessary for each bus to consider the power flow:

- P_k—active power

- V_k—voltage magnitude

There are two kinds of bus definitions:

- Voltage-controlled bus (V-node),

- Power-controlled bus (P-node).

The voltage and power injection are maintained at a given value at this bus. The DC network equation, without considering the model of DC-DC converters, can be expressed as follows:

$$P_k = \sum_m V_k V_m G_{km} \qquad (10)$$

In order to solve power flow equations, using the N-R method, we need to form differentials that relate linearly small variations in V to small variations in P as follows:

$$\Delta P_k = \sum_m \frac{\partial P_k}{\partial V_m} \Delta V_m \qquad (11)$$

Equation (11) can be extended to the whole system as [18]:

$$[\Delta P] = [J^{dc}] \cdot [\Delta V]$$

$[J^{dc}]$ is a Jacobian matrix which is formed for a DC network. It is an $N \times N$ matrix (N is the number of p-node buses). The elements in the Jacobian matrix are given by:

$$J_{km}^{dc} = \frac{\partial P_k}{\partial V_m} = \begin{cases} V_k G_{km} & m \neq k \\ \frac{P_k}{V_k} + V_k G_{kk} & m = k \end{cases} \qquad (12)$$

4. Incorporating DC-DC Converters

4.1. Modeling of DC-DC converters

Suppose a DC-DC converter is located between nodes i and j in a DC network (as shown in Fig. 1). Node i is supposed as the voltage controlled node.
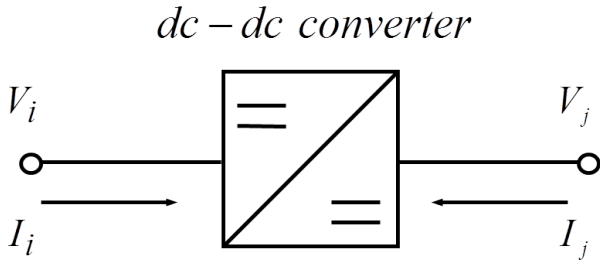
$dc - dc$ converter

Figure 1: A DC-DC converter model [18]

DC-DC converter is modeled for power flow analysis taking into account power losses and control strategy as [18]:

$$P_i = \sum_{m \neq j} V_i V_m G_{im} + V_i I_i \qquad (13)$$

$$P_j = \sum_{m \neq i} V_j V_m G_{jm} + V_j I_j \qquad (14)$$

$$E = V_i I_i + V_j I_j - P_{loss} = 0 \qquad (15)$$

$$V_i = V^{spec} \qquad (16)$$

where: P_i, P_j—the nodal power at node i and j, G_{xm}—the element (x, m) in the bus admittance matrix, E—the power balance equation, P_{loss}—the power losses of the DC-DC converter, V^{spec}—the expected voltage value at node i.

The control method of the converter is specified by (16). The loss of the DC-DC converter P_{loss} is obtained from (1).

4.2. Modified DC power flow

The power flow model of DC-DC converters are integrated into the DC power flow algorithm by changing the formation of Jacobian matrix $[J^{dc}]$ [18]. At first, form the $N \times N$ Jacobian matrix $[J^{dc}]$ without counting the DC-DC converters; in other words open circuit the DC-DC converter. The nodes i and j are considered as V-node and P-node respectively. Then, include all the DC-DC converters modifying $[J^{dc}]$.

- Step 1: Two variables shall be added for each DC-DC converter: I_i and I_j. Then the iteration variables become $[V_1 \dots V_N \quad I_i^1 \dots I_i^{Ncon} \quad I_j^1 \dots I_j^{Ncon}]$. Consequently, $2 \times N_{con}$ columns will be added into $[J^{dc}]$, whose values are all zero initially.

- Step 2: The right node of each DC-DC converter has already been specified as P-node. However, the power flow of the DC-DC converter has not been included in the power equation. The actual nodal power is given by (14). Therefore, the j-th row of $[J^{dc}]$ shall be modified at row j and column $N + N_{con} + n$ to put the differential values of P_j with respect to V_j and I_j (based on (14)). i and j are related to n-th converter as $n = \{1 \dots N_{con}\}$.

- Step 3: Based on the nodal power equation specified in (13), a new row related to ΔP_j for each converter can be added into $[J^{dc}]$ (in rows $N + n$). The differential values of P_j with respect to voltage $V_1 \dots V_N$ and I_i are obtained from (13). The dimensions of the new modified Jacobian matrix are $N + N_{con}$ and $N + 2 \times N_{con}$ respectively.

The differentials can be obtained as:

$$\frac{\partial P_i}{\partial V_m} = V_i G_{im} \quad for \quad m = 1 \dots N \qquad (17)$$

- Step 4: An additional row representing the power balance equation (15) for n-th converter is added into the matrix $[J^{dc}]$ (in row $N + N_{con} + n$). For each converter, differentials of E with respect to V_j, I_i and I_j are obtained and are added in row $N + N_{con} + n$ and columns j, $N + n$, $N + N_{con} + n$, respectively. This is repeated for each converter and finally we have a Jacobian matrix with dimensions $(N + 2 \times N_{con})$ and $(N + 2 \times N_{con})$.

The differentials can be obtained as:

$$\frac{\partial E}{\partial V_j} = I_j - \frac{\partial P_{loss}}{\partial V_j} \qquad (18)$$

$$\frac{\partial E}{\partial I_i} = V_i - \frac{\partial P_{loss}}{\partial I_i} \qquad (19)$$

$$\frac{\partial E}{\partial I_j} = V_j - \frac{\partial P_{loss}}{\partial I_j} \qquad (20)$$

The partial derivatives of P_{loss} in (18)–(20) can be obtained from (1)–(8). The results are given in appendix A.

The power flow equation regarding the new Jacobian matrix is given by:

$$\begin{bmatrix} \Delta P \cdots \Delta P_N & \Delta P_i^1 \cdots \Delta P_i^{N_{con}} & E^1 \cdots E^{N_{con}} \end{bmatrix}^T =$$
$$\begin{bmatrix} J^{dc+} \end{bmatrix} \begin{bmatrix} V \cdots V_N & I_i^1 \cdots I_i^{N_{con}} & I_j^1 \cdots I_j^{N_{con}} \end{bmatrix}^T \qquad (21)$$

$$J_{km}^{dc} = \frac{\partial P_k}{\partial V_m} = \begin{cases} V_k G_{km} & m \neq k \\ \frac{P_k}{V_k} + V_k G_{kk} & m = k \end{cases} \qquad (22)$$

The previous work on DC-DC boost converter modeling had some deficiencies in equations 31, 34 and 36, which are modified as in appendix 8.1.

5. Modeling of Wind Power Generation

Wind speed has an uncertain nature which can be modeled by a probability function. The Weibull distribution function has been used to represent wind speed modeling [21]. The Weibull probability density function is as follows:

$$f_v(v) = \begin{cases} \frac{\beta}{\alpha} \left(\frac{v}{\beta} \right)^{\beta - 1} \times \exp \left(- \left(\frac{v}{\alpha} \right)^{\beta} \right) & v \geq 0 \\ 0 & otherwise \end{cases} \qquad (23)$$

where, α and β are the shape and scale parameters of the Weibull distribution function and v is the wind speed in [m/s].

The wind speed is converted into power as (24):

$$P_{G,WT}(v) = \begin{cases} P_{r,WT} \cdot \left(\frac{v_{cut-in}^2 - v^2}{v_{cut-in}^2 - v^2} \right) & v_{cut-in} \leq v \leq v_r \\ P_{r,WT} & v_r \leq v \leq v_{cut-out} \\ 0 & otherwise \end{cases} \quad (24)$$

where $P_{r,WT}$ is the rated power of wind turbine in kW, v_{cut-in} and $v_{cut-out}$ are the wind turbine cut-in and cut-out speeds in m/s, and v_r is the rated speed of wind turbine in m/s. A number of samples based on Weibull distribution are generated. The presented DC power flow is used to analyze the steady-state condition of the network for every sample wind power generation.

6. Numerical Example

The algorithm presented above is tested on a system containing 51 buses, 40 short cables and one long distance cable, 40 wind turbines (WT) and 10 DC-DC boost converters as in Fig. 2. The WTs are composed of a synchronous generator followed by a rectifier. The inverter connected to bus 51 maintains the DC voltage. Therefore, bus 51 is considered as V-node, while the wind turbines are considered as P-node. The parameters of the system elements are given in Table 1 of appendix 8.2.

6.1. Validation

The load flow algorithm presented in [18] is re-worked in this paper. In order to validate this paper the results are given. At this stage, the wind speed is set so that each WT generates the rated power.

Based on the method presented in previous sections, power flow analysis is performed. Fig. 3 shows the flowchart of the algorithm. The value for parameter ε as a stopping criterion is 0.0001. The calculation converged in 4 iterations. The voltage magnitudes are given in Table 1 and are compared with the previous work [18]. The differences are subtle. It should be noted that the values of some parameters were not given in [18]: initial values for power flow analysis are given in Fig. 3 and curve fitting parameters are given in Table 1. The voltage profile can also be seen in Fig. 4.

6.2. Uncertainty in wind power

As an application of the DC-DC converter model in load flow analysis and in order to show the robustness of the algorithm, wind power is assumed to be uncertain, which is necessary in real studies. As presented in section 5, 10000 wind speed samples are generated based on the Weibull distribution function with the parameters $\alpha = 2$ and $\beta = 7$. The density figure of wind speed is as Fig. 5. In order to show the results statistically, normal fit of density figures are given over the density bars. In every sample the wind speed is assumed to be similar for all the wind turbines in the wind farm.

For every sample a power flow analysis is performed. The parameters used for wind power generations based on equation (24) are as follow:

$$P_{r,WT} = 2.5\,\text{MW} \qquad v_r = 12\,\text{m/s}$$
$$v_{cut-in} = 2.5\,\text{m/s} \qquad v_{cut-out} = 30\,\text{m/s}$$

The density figure of wind power generation is shown in Fig. 6. As an example, the density figure of losses in a boost converter is shown in Fig. 7 in which for all the samples the average value of loss is 0.06 MW and the variance is 0.05 MW.

7. Conclusion

The purpose of this paper is to shed light on the importance of incorporating models of PEIs into power flow studies. So, the precise modeling of a DC-DC boost converter for power flow analysis was presented. As an application the model was employed in an uncertainty study of wind power generation and the results demonstrate the robustness of the algorithm. The model can be used for various other applications, ranging from planning to operation studies. Conventional distribution networks are evolving into smart distribution networks, and DC-DC converters as a kind of PEIs are mostly incorporated in the smart grid environment.

8. Appendices

8.1. The partial derivatives of P_{loss} in the boost converter

$$\frac{\partial D_x}{\partial V_j} = 0 \quad (25)$$

$$\frac{\partial D_x}{\partial I_i} = -(R_L + R_{o,sw}) \quad (26)$$

$$\frac{\partial D_y}{\partial V_j} = 1 \quad (27)$$

$$\frac{\partial D_y}{\partial I_i} = R_{o,D} - R_{o,sw} \quad (28)$$

$$\frac{\partial D_z}{\partial V_j} = 1 \quad (29)$$

$$\frac{\partial D_z}{\partial I_i} = R_L + R_{o,D} \quad (30)$$

$$\frac{\partial D}{\partial V_j} = \frac{LI_i}{DD_x D_y^2 T_s} \left(D_y - D_z \right) \quad (31)$$

$$D_{\Sigma} = D + D' \quad (32)$$

$$\frac{\partial D_{\Sigma}}{\partial V_j} = \frac{-2LI_{in}}{T_s D_x D^2} \frac{\partial D}{\partial V_j} \quad (33)$$

$$\frac{\partial D}{\partial I_i} = -\frac{LI_i}{T_s DD_x^2 D_y^2} D_z \left(\frac{\partial D_x}{\partial I_i} D_y + \frac{\partial D_y}{\partial I_i} D_x \right) \quad (34)$$
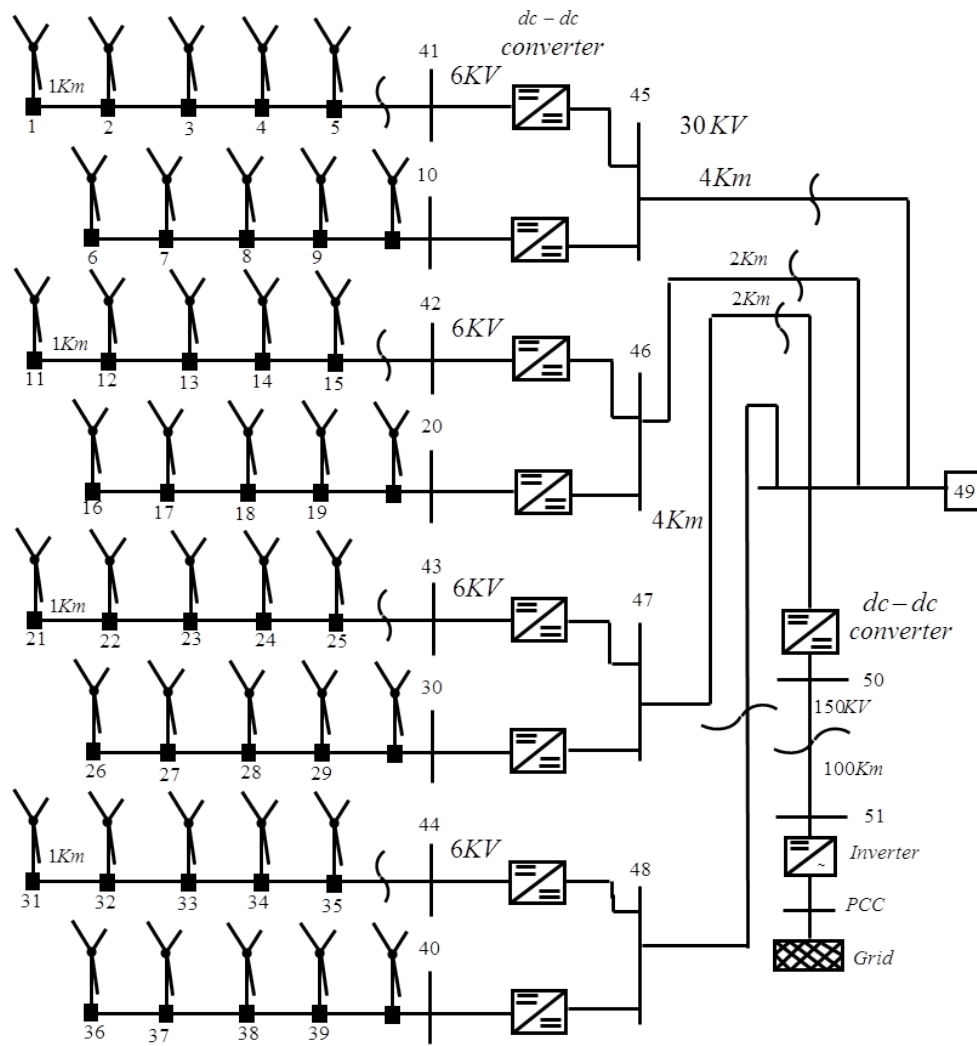
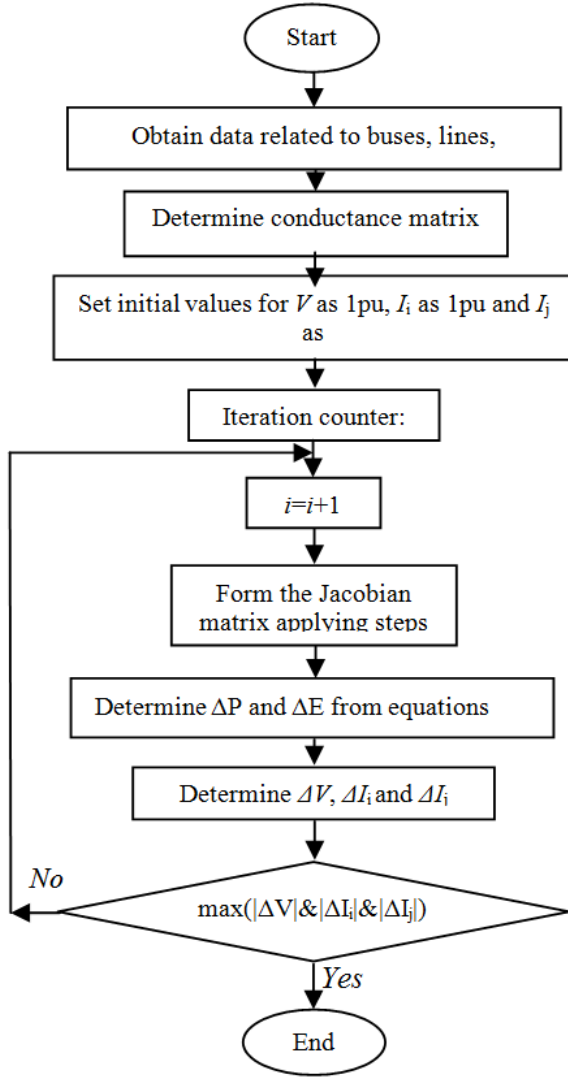Figure 2: An offshore wind farm electrical system with DC network [18]
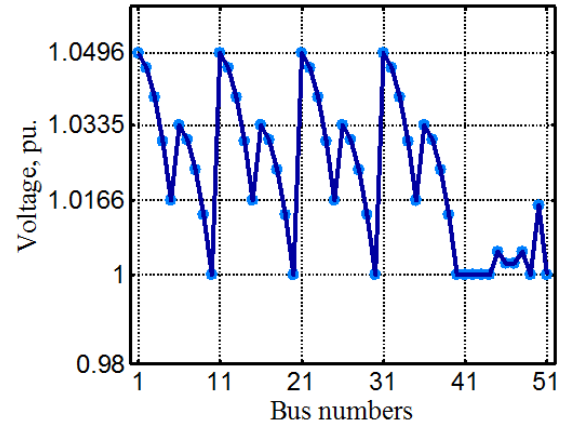
Figure 3: Flowchart of the presented power flow algorithm

Figure 4: Voltage profile of the system after power flow analysis
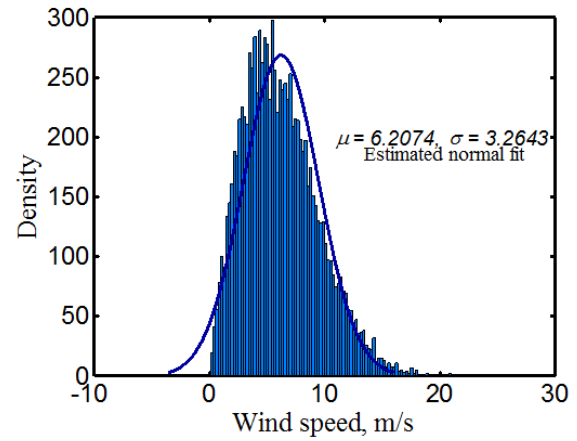
Figure 5: Density of wind power generated by one of the WTs

$$\frac{\partial \frac{D}{D_\Sigma}}{\partial V_j} = \frac{1}{D_\Sigma^2}\left(D_\Sigma \frac{\partial D}{\partial V_j} - D\frac{\partial D_\Sigma}{\partial V_j}\right) \tag{35}$$

$$\frac{\partial D_\Sigma}{\partial I_i} = \frac{-2LI_i}{T_s D_x^2 D^2}\left(D\frac{\partial D_x}{\partial I_i} - D_x \frac{\partial D}{\partial I_i}\right) \tag{36}$$

$$\frac{\partial \frac{D}{D_\Sigma}}{\partial I_i} = \frac{1}{D_\Sigma^2}\left(D_\Sigma \frac{\partial D}{\partial I_i} - D\frac{\partial D_\Sigma}{\partial I_i}\right) \tag{37}$$

$$\frac{\partial P_{loss}}{\partial V_j} = I_i\left(\frac{A_{on,sw}+A_{off,sw}}{T_s} + \frac{A_{rec,D}}{T_s}\right) + [V_{o,sw} + R_{o,sw}I_i - V_{o,D} - R_{o,D}I_i] I_i \frac{\partial \frac{D}{D_\Sigma}}{\partial V_j} \tag{38}$$

$$\frac{\partial P_{loss}}{\partial I_i} = 2R_L I_i + [V_{o,sw} + R_{o,sw}I_i - V_{o,D} - R_{o,D}I_i] I_i \frac{\partial \frac{D}{D_\Sigma}}{\partial I_i} + V_j\left(\frac{A_{on,sw}+A_{off,sw}}{T_s} + \frac{A_{rec,D}}{T_s}\right) + \frac{D}{D+D'}\left(V_{o,sw} + 2R_{o,sw}I_i\right) + \frac{D'}{D+D'}\left(V_{o,D} + 2R_{o,D}I_{in}\right) \tag{39}$$

$$\frac{\partial P_{loss}}{\partial I_j} = 0 \tag{40}$$

8.2. Test system parameters

Table 1: Parameters of the Test System

| Devices	Parameters	Values
wind turbines [18]	Rating of WT, MW	2
	Voltage of WT, kV DC	6
	Type of generator	PMSG
Dc cables [18]	Resistance of 6 kV DC cable, Ω/km	0.062
	Resistance of 30 kV DC cable, Ω/km	0.06
	Resistance of 150 kV DC cable, Ω/km	0.047
6/30 kV DC-DC converter [18]	Switching frequency, kHz	2
	Voltage drop of IGBT, kV	0.00684
	Resistance of IGBT, Ω	0.0068
	Voltage drop of diode, kV	0.00498
	Resistance of diode, Ω	0.0039
	Inductance, mH	8
	Resistance of inductor, Ω	0.001
30/150 kV DC-DC converter [18]	Switching frequency, kHz	1
	Voltage drop of IGBT, kV	0.034
	Resistance of IGBT, Ω	0.021
	Voltage drop of diode, kV	0.025
	Resistance of diode, kV	0.0122
	Inductance, mH	18
	Resistance of inductor, Ω	0.002
Others [18]	Base value for frequency, Hz	50
	Base for power, MVA	100
Curve fitting parameters [20]	$A_{sw,on}$	11.67×10^{-7}
	$A_{sw,off}$	8.33×10^{-7}
	$A_{rec,D}$	5.42×10^{-7}
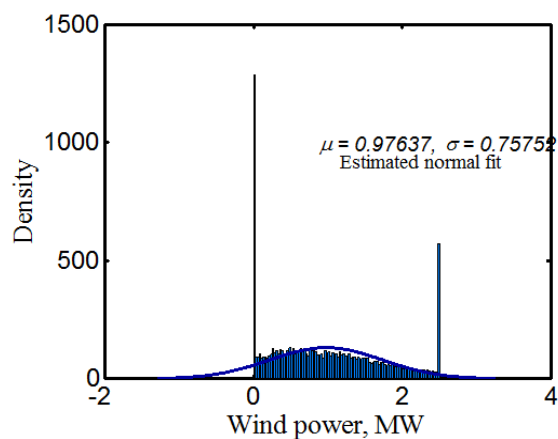
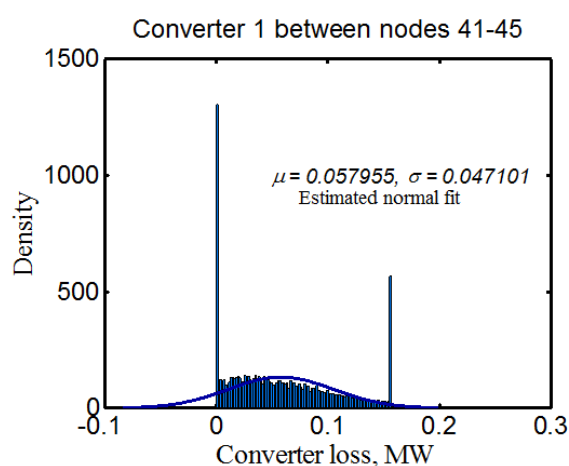Figure 6: Density of wind power generated by one of the WTs

Figure 7: Density of losses in the converter between nodes 41--45

References

[1] S. A. Mohammed, M. Abdel-Moamen, B. Hasanin, A review of the state-of-the-art of power electronics for power system applications, Quest Journal of Electronics and Communication Engineering Research (JECER) 1 (1) (2013) 43–52.

[2] C. Meyer, R. W. De Doncker, Power electronics for modern medium-voltage distribution systems, in: Power Electronics and Motion Control Conference, 2004. IPEMC 2004. The 4th International, Vol. 1, IEEE, 2004, pp. 58–66.

[3] T. Kaipia, P. Peltoniemi, J. Lassila, P. Salonen, J. Partanen, Power electronics in smartgrids-impact on power system reliability, in: CIRED Seminar 2008 Smart Grids for Distribution, paper no. 0124, 2008, pp. 83–83.

[4] F. Blaabjerg, Z. Chen, S. B. Kjaer, Power electronics as efficient interface in dispersed power generation systems, IEEE transactions on power electronics 19 (5) (2004) 1184–1194.

[5] J. M. Carrasco, L. G. Franquelo, J. T. Bialasiewicz, E. Galván, R. C. PortilloGuisado, M. M. Prats, J. I. León, N. Moreno-Alfonso, Power-electronic systems for the grid integration of renewable energy sources: A survey, IEEE Transactions on industrial electronics 53 (4) (2006) 1002–1016.

[6] Z. Chen, J. M. Guerrero, F. Blaabjerg, A review of the state of the art of power electronics for wind turbines, IEEE Transactions on power electronics 24 (8) (2009) 1859–1875.

[7] S. B. Kjaer, J. K. Pedersen, F. Blaabjerg, A review of single-phase grid-connected inverters for photovoltaic modules, IEEE transactions on industry applications 41 (5) (2005) 1292–1306.

[8] A. Kirubakaran, S. Jain, R. Nema, A review on fuel cell technologies and power electronic interface, Renewable and Sustainable Energy Reviews 13 (9) (2009) 2430–2440.

[9] D. Divan, H. Johal, Distributed facts—a new concept for realizing grid power flow control, IEEE Transactions on Power Electronics 22 (6) (2007) 2253–2260.

[10] M. Sabahi, A. Y. Goharrizi, S. H. Hosseini, M. B. B. Sharifian, G. B. Gharehpetian, Flexible power electronic transformer, IEEE Transactions on Power Electronics 25 (8) (2010) 2159–2169.

[11] X. Wang, J. M. Guerrero, F. Blaabjerg, Z. Chen, A review of power electronics based microgrids, Journal of Power Electronics 12 (1) (2012) 181–192.

[12] O. Zavalani, M. Braneshi, A. Spahiu, L. Prifti, Potentials of power electronics in LV electricity distribution systems in Albania, in: Power Electronics and Motion Control Conference (EPE/PEMC), 2010 14th International, IEEE, 2010, pp. 59–64.

[13] M. Hosseini, H. Shayanfar, M. Fotuhi-Firuzabad, Modeling of unified power quality conditioner (UPQC) in distribution systems load flow, Energy Conversion and Management 50 (6) (2009) 1578–1585.

[14] M. Farhoodnea, A. Mohamed, H. Shareef, H. Zayandehroodi, Optimum placement of active power conditioner in distribution systems using improved discrete firefly algorithm for power quality enhancement, Applied Soft Computing 23 (2014) 249–258.

[15] P. A. N. Garcia, J. L. R. Pereira, S. Carneiro, Voltage control devices models for distribution power flow analysis, IEEE Transactions on Power Systems 16 (4) (2001) 586–594.

[16] P. Yan, A. Sekar, Analysis of radial distribution systems with embedded series FACTS devices using a fast line flow-based algorithm, IEEE Transactions on Power Systems 20 (4) (2005) 1775–1782.

[17] M. Z. Kamh, R. Iravani, A unified three-phase power-flow analysis model for electronically coupled distributed energy resources, IEEE Transactions on Power Delivery 26 (2) (2011) 899–909.

[18] M. Zhao, Z. Chen, F. Blaabjerg, Modeling of DC/DC converter for DC load flow calculation, in: Power Electronics and Motion Control Conference, 2006. EPE-PEMC 2006. 12th International, IEEE, 2006, pp. 561–566.

[19] M. Zhao, Z. Chen, F. Blaabjerg, Load flow analysis for variable speed offshore wind farms, IET Renewable Power Generation 3 (2) (2009) 120–132.

[20] S. Lundberg, Performance comparison of wind park configurations, Tech. rep., Chalmers University of Technology (2003).

[21] N. Nikmehr, S. N. Ravadanegh, Optimal power dispatch of multi-microgrids at future smart distribution grids, IEEE Transactions on Smart Grid 6 (4) (2015) 1648–1657.